RNA (2001), *7*:598–609. Cambridge University Press. Printed in the USA.

A short fragment of 23S rRNA containing the binding sites for two ribosomal proteins, L24 and L4, is a key element for rRNA folding during early assembly

ULRICH STELZL and KNUD H. NIERHAUS

Max-Planck-Institut für Molekulare Genetik, AG Ribosomen, D-14195 Berlin, Germany

ABSTRACT

Previously we described an in vitro selection variant abbreviated SERF (in vitro selection from random rRNA fragments) that identifies protein binding sites within large RNAs. With this method, a small rRNA fragment derived from the 23S rRNA was isolated that binds simultaneously and independently the ribosomal proteins L4 and L24 from *Escherichia coli*. Until now the rRNA structure within the ternary complex L24–rRNA–L4 could not be studied due to the lack of an appropriate experimental strategy. Here we tackle the issue by separating the various complexes via native gel-electrophoresis and analyzing the rRNA structure by in-gel iodine cleavage of phosphorothioated RNA. The results demonstrate that during the transition from either the L4 or L24 binary complex to the ternary complex the structure of the rRNA fragment changes significantly. The identified protein binding sites are in excellent agreement with the recently reported crystal structure of the 50S subunit. Because both proteins play a prominent role in early assembly of the large subunit, the results suggest that the identified rRNA fragment is a key element for the folding of the 23S RNA during early assembly. The introduced in-gel cleavage method should be useful when an RNA structure within mixed populations of different but related complexes should be studied.

Keywords: iodine cleavage; phosphorothioate modification; ribosomal assembly; ribosomes; RNA–protein interaction; structural probing

INTRODUCTION

The RNA structure within ribonucleo-protein particles (RNPs) might deviate strongly from that observed with free RNA. For example, the ribosomal assembly runs through a series of intermediate particles with increasing S-values. Thus, the folding process leads to particles of increasing compactness during the course of assembly involving conformational changes of the rRNA, although the number of proteins present in the intermediates successively formed goes up (for review see Nierhaus, 1991). The structural changes of the rRNAs during the assembly process are an interesting issue, but suitable techniques to study this issue are rare. It is prohibitively difficult to follow the folding process by X-ray analysis, because the intermediate particles have a looser structure than the mature particle, thus impeding the formation of crystals. Likewise, NMR methods cannot be applied, because complexes involving more than three RNA or protein components are usually too large to be analyzed. Digestion experiments of the RNPs with RNases specific for single or double strands are not informative, because internal RNA regions are not accessible to the enzymes. Hydroxyl radicals or reagents that modify bases in single-stranded regions are small enough to penetrate a complex and to give valuable information about RNA binding sites of proteins. These techniques have been successfully applied for the assembly of the small subunit of the *Escherichia coli* ribosome (Powers et al., 1993; Powers & Noller, 1995), where proteins were added one by one according to the 30S assembly map. Nucleotides that were accessible in the preceding assembly step but became protected upon addition of the next protein allowed conclusions about the effects of this protein.

Another important technique is the phosphorothioate technique (Verma & Eckstein, 1998; Strobel, 1999), where modified RNAs that contain a sulfur atom in-

Reprint requests to: Knud H. Nierhaus, Max-Planck-Institut für Molekulare Genetik, AG Ribosomen, Ihnestrasse 73, D-14195 Berlin, Germany; e-mail: nierhaus@molgen.mpg.de.

Abbreviations: αS-RNA, phosphorothioated RNA; PAGE, polyacrylamide gel electrophoresis; RNP, ribonucleo-protein; $rRNA^{L4}$, GG283–U358 rRNA fragment from domain I of 23S rRNA (77 nt).

stead of a nonbridging oxygen at the phosphate residues are used. The small inert iodine can trigger a cleavage of the phosphate-sugar backbone at the modified phosphate residue (Gish & Eckstein, 1988) and thus probe the structure based on accessibility. The advantage of this method is that it works equally well in single- and double-stranded RNA regions; in addition the modified RNA usually has full biological activity, as demonstrated for thioated tRNAs (Rudinger et al., 1992; Dabrowski et al., 1995).

In some cases the incorporation of single thioated nucleotides prevents, for example, formation of an RNA–protein complex. A reason could be that either a phosphorothioate at this position can induce a change of the RNA structure that prevents binding (Smith & Nikonowicz, 2000) or the unmodified phosphate at this position is essential for complex formation. This experimental strategy to identify residues essential for binding is called interference strategy, because modifications that interfere with the complex formation are identified. The remaining majority of nucleotides do not interfere with complex formation and thus can be analyzed in a second strategy of this method, namely, the protection approach. Here the extent of protection against iodine cleavage by the proteins in complex with RNA can be assessed thus revealing contacts with the respective phosphate residues.

The effects of phosphorothioate modification on RNA–protein interaction match direct structural information obtained from corresponding X-ray structures or that derived by cryoelectron microscopy very well. For example, results obtained with the MS2 coat protein–RNA (Milligan & Uhlenbeck, 1989; Dertinger et al., 2000) and tRNA–synthetase systems (Schatz et al., 1991; Rudinger et al., 1992; Voertler et al., 1998) are directly comparable to interactions seen in three-dimensional crystal structures of the complexes. Phosphorothioated tRNAs bound by the ribosome give specific cleavage patterns that are characteristic for the particular ribosomal binding site (Dabrowski et al., 1995) and that are dependent on the functional state of the ribosome (Dabrowski et al., 1998). The protection pattern observed with P-site bound peptidyl–tRNA analogs was in perfect agreement with the ribosome contacts seen with an f-Met-tRNA at the ribosomal P site in cryoelectron microscopy pictures (Malhotra et al., 1998).

Recently, we selected a short fragment of domain I of 23S rRNA (GG295–343CC, 53 nt) that binds independently and simultaneously the ribosomal proteins L4 and L24 (Stelzl et al., 2000a, 2000b), two key proteins for the early assembly of the large subunit of bacterial ribosomes (Nierhaus, 1991). L24 is one of the two assembly initiator proteins of the 50S subunit (Nowotny & Nierhaus, 1982), and L4 is essential for the formation of the first assembly intermediate particle (Spillmann et al., 1977). Here, we present phosphorothioate probing data of the ternary L24–rRNA–L4 complex determined by an in-gel analysis and compare them with that of the two binary complexes L24–rRNA and rRNA–L4. In-gel iodine cleavage enables the probing of RNA structures in homogeneous populations of the different complexes, thereby overcoming the problem that a preparation of a ternary complex still contains a fraction of binary complexes obscuring the signals. The results demonstrate that the rRNA region within the binary complexes adopts a conformation that is different from that observed in the ternary complex. We discuss these probing data in light of the recent crystallographically determined three-dimensional model of the 50S ribosomal subunit (Ban et al., 2000).

RESULTS

Iodine cleavage within native gels

Both ribosomal proteins L4 and L24 bind independently and simultaneously to a 53-nt rRNA fragment of domain I in 23S rRNA (GGG295–C343CC) with μM^{-1} affinities (Stelzl et al., 2000a). The rRNA in the two corresponding binary complexes was characterized by phosphorothioate cleavage; the complexes were separated from the nonbound rRNA fragments by nitrocellulose filtration.

The approach works well for binary RNA–protein complexes but not for the ternary L4–rRNA–L24 complex, if nitrocellulose filtration is used. A mixture of all three complexes is retained by nitrocellulose filtration, which masks the signal of the ternary complex. In addition, it is difficult to separate each of the complexes due to the fact that they differ only by about 11 kDa in size (L24–rRNA–L4: 51.2 kDa; rRNA–L4 40.0 kDa; L24–rRNA: 29.1 kDa). If the rRNA were to have a different conformation in the ternary complex as compared to either of the binary complexes, the signals would be weakened or even masked by the contaminating binary complexes.

We have solved this problem by probing the RNA–protein complexes within native gels (Fig. 1). Approximately one α-phosphorothioate per molecule is introduced via T7 in vitro transcription 5′ to either an A, C, G, or U nucleotide into the rRNA fragment. These RNAs are further 5′-[^{32}P]-labeled and used for complex formation with the proteins. Free RNA and the complexes are subjected to native gel electrophoresis, where each species migrates at a defined position (Fig. 1B). The bands are localized by autoradiography and cut out from the gels. Subsequently, each band is treated in one of the following ways depending on the experimental strategy to be applied (Fig. 1A): (1) In the course of an *interference experiment*, the RNA is extracted from the complex out of the gel piece and subsequently cleaved with iodine under denaturating conditions (7 M urea). A band that is *weakened or missing* in the following sequencing gel indicates the absence of a certain modification in the RNA–protein

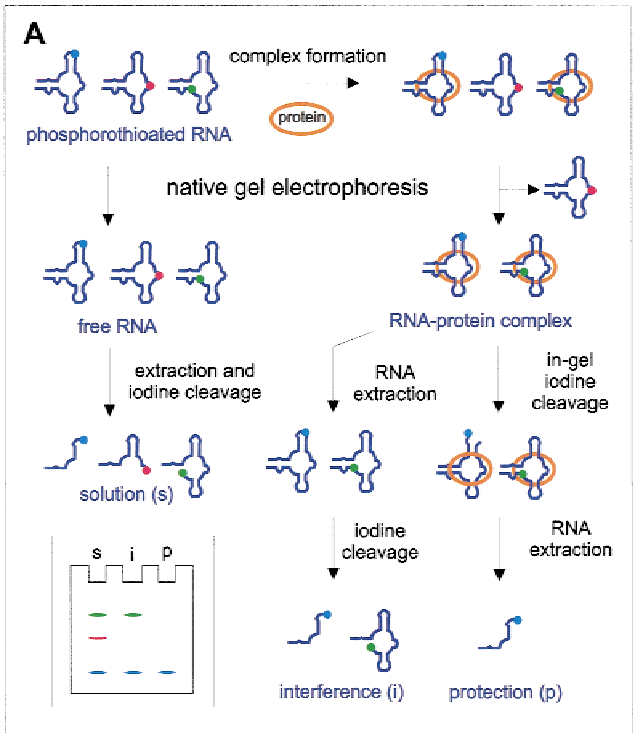

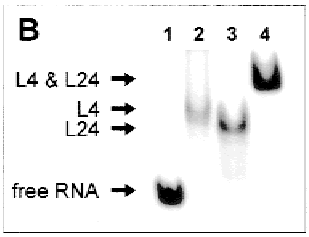

FIGURE 1. A: Outline of the in-gel cleavage experiments. Free αS-RNA and αS-RNA in complex with proteins is subjected to native gel electrophoresis (cf. **B**). The complexes are localized in the gel and either cleaved with iodine in-gel (right, p) or after extraction from the gel (middle, i). Free RNA is treated as a comparison (left, s). The cleavage products are analyzed on a sequencing gel (insert). For data quantification, intensities of the corresponding bands are compared: interference = i/s; protection = p/i. **B:** Band-shift assay with RNA^{L4} (77 nt) and ribosomal proteins L4 and L24: 6% polyacrylamide-gel buffered with 20 mM HEPES-KOH (pH 7.4 at 0 °C), 4 mM $MgCl_2$, 100 mM NH_4Cl. Lane 1: free RNA^{L4}; lane 2: L4 and $rRNA^{L4}$; lane 3: L24 and $rRNA^{L4}$; lane 4: L4, L24, and $rRNA^{L4}$.

complex. In other words, the presence of a thioate at a particular position impedes or interferes with binding. The opposite is also observed, namely that a band is *stronger* than in the control. This means that a phosphorothioate at this position is present in a larger fraction within the complex than in the initial αS-RNA pool, that is, this phosphorothioate increases the affinity between the rRNA fragment and the protein, thus leading to an enrichment of this fragment within the complex. (2) In a *protection experiment*, the RNA is cleaved in the complex within the nondenaturing gel; the gel piece is soaked with 3 mM iodine in binding buffer for 10–15 min on ice, and the cleavage reaction is quenched by reducing the iodine with dithiothreitol (in-gel cleavage). As soon as the in-gel cleavage reaction is stopped, the RNA is extracted from the gel piece and the RNA cleavage products are separated on a sequencing gel. A *weakened or absent* band in this experiment indicates that iodine does not have free access to the backbone of the RNA in this region, that is, the position is protected from iodine cleavage. The alternative, a *stronger* band, also occurs, meaning that the phosphorothioate at this position is more exposed (more reactive) to the iodine within the complex than in the naked fragment.

In-gel cleavage of free RNA does not show many differences in the cleavage intensities as compared to free RNA that is extracted from the gel before iodine cleavage under denaturing conditions (average relative intensity is 1.01 $\pm$ 0.26; not shown). Three exceptions are observed: Apparently, U293 cannot be cleaved within the gel, as the band for U293 is missing in the in-gel-cleavage experiments (cf. Fig. 4). Statistically, cleavage of A320 is pronounced (relative intensity 1.73), whereas the intensity of the band A340 is reduced (relative intensity 0.44) when cleaved in the gel.

The L4–rRNA and L24–rRNA complexes: In-gel cleavage versus nitrocellulose filter technique

In the following, we describe the binding of the two proteins, L4 and L24, to the fragment $rRNA^{L4}$ with a length of 77 nt (Fig. 2A). The initial G of this GG283–U358 fragment ($rRNA^{L4\text{-}2}$ in Stelzl et al., 2000a) is not derived from the rRNA sequence, but is due to transcription requirements. We do not use the minimal 53-nt fragment ($rRNA^{L4\text{-}3}$ in Stelzl et al., 2000a), because the corresponding complexes with the longer RNA^{L4} fragment separate well in gel electrophoresis (Fig. 1B), significantly better than the complexes with the smaller rRNA fragment (not shown). Both fragments have the same protein binding capabilities (Stelzl et al., 2000a).

Nitrocellulose filtration is a nonequilibrium method for measuring binding affinities, the separation of the complex from the noncomplexed molecules requires several seconds. The respective situation in gel-shift experiments is more harsh, because the electrophoresis lasts 2 h under our conditions, and weakly bound RNA molecules are removed from the complex. As a consequence, the apparent association constants are usually smaller (up to one order of magnitude), when measured via gel shift as compared to nitrocellulose filter measurement (Draper et al., 1988). It follows that the more stringent method, namely, the gel-shift experiment, changes the pattern in the direction of higher binding selectivity. This is indicated by the following observations. (1) When we compare the filtration results of the two binary complexes with those of in-gel cleavage, clearly more O-to-S substitutions affect bind-

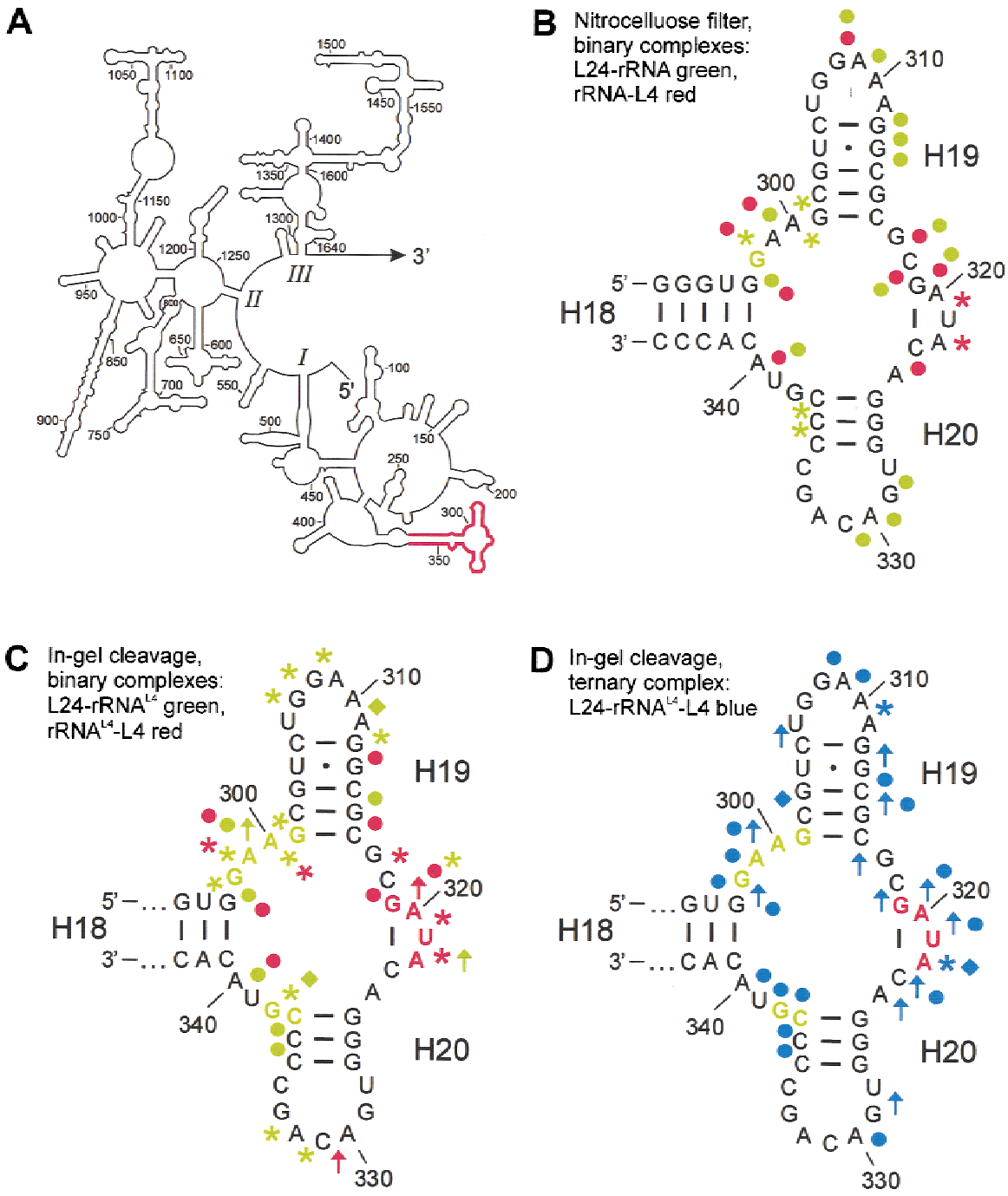

FIGURE 2. **A:** Secondary structure of the 5′ half of *E. coli* 23S rRNA (1–1646). The $rRNA^{L4}$ fragment used is indicated in red (GG283–U358, 77 nt). **B–D:** Iodine cleavage pattern projected onto the rRNA secondary structure. Intensities of bands that differ by a factor of 1.5 from the comparison are indicated: ∗ decreased and ↑ increased binding (from interference experiments); ● decreased and ♦ enhanced cleavage in the complex (from protection experiments). **B:** Cleavage patterns of the binary complexes as seen with the nitrocellulose filter technique, L24–rRNA in green and rRNA–L4 in red; A G298U (green nucleotide) mutation abolishes L24 binding (Stelzl et al., 2000a). **C:** Cleavage patterns as seen with in-gel cleavage technique; nucleotide positions interacting with L24 and L4 are highlighted in green and red, respectively. **D:** In-gel probing results of the L24–$rRNA^{L4}$-L4 ternary complex (blue).

ing of the proteins in the band-shift approach (Fig. 2C shows more stars than Fig. 2B). Several positions, mainly in the loop of helices H19 and H20, interfere with binding of L24 (green stars) according to the gel-shift experiment but not in the filtration experiment: 5′ to G307, G308 in H19, A320 and 5′ to A332 and G333 in H20. In the in-gel cleavage experiment, a thioate at G301 interferes with L4 binding (red stars). (2) In the band-shift experiment, four positions with a phosphorothioate modification were enriched in the complexes

(arrows in Fig. 2C), that is, the substitutions favor the binding of the protein as compared to the nonmodified molecules. An oxygen-to-sulfur substitution at A300 and A322 stimulates binding of L24 (green arrows); a similar effect is seen for positions A320 and C331 in the case of protein L4 (red arrows).

Protection experiments reflect the accessibility of the RNA backbone for iodine within the RNA–protein complex. Some protections seen in the filter assays do not show up in the gel-shift assay (e.g., circles around A330 in Fig. 2B but not in 2C), and a few protection signals are even replaced by interference signals (A309, G312, and A320 in the case of L24, A299, and C318 for L4) in the gel-shift approach. Binding of L24 exposes A311 and G338 to I_2 cleavage in the complex within the gel (Fig. 2C, diamonds).

Based on the nitrocellulose filter probing results in the previous analysis (Stelzl et al., 2000a), the RNA regions directly interacting with the proteins were tentatively assigned. Despite the apparent differences of the patterns caused by the two techniques, the probing data within these regions are exactly the same. The L4 interaction site is the sequence G319–A322 (red in Fig. 2C). The phosphate backbone connections 5′ to G319 and A320 are protected from cleavage in the complex and the O-to-S backbone substitutions at U321 and A322 impede binding of L4. The cleavage pattern of this region is shown in Figure 3A. The L24 interaction site is located in both the G298–G301 and the C337–G338 region (green in Fig. 2C). The cleavage pattern in the first region is the same in both approaches, that is, G298 and A300 are strongly protected from iodine cleavage by L24, and phosphorothioates at A299, G301, and C302 interfere with binding of the protein (this gel section is shown in Fig. 3B). In the second region, however, the pattern is changed: the G338 substitution is underrepresented but exposed to cleavage in the complex, and the C334–C337 signal is reduced in the complex with L24.

The probing results obtained by the two techniques clearly define two distinct regions of interaction. The L4 interaction site is centered around nucleotide U321, the L24 binding site is around A299 plus C337–G338 on the opposite strand in the three helix junction.

Structural probing of the L24–rRNA–L4 ternary complex

The in-gel cleavage approach not only gives a detailed look into the L24–rRNA and the rRNA–L4 interactions, but provides the first means to probe the ternary L24–$rRNA^{L4}$–L4 complex in a defined way, that is, without signal impairment due to contamination of binary complexes. A representative gel is given in Figure 4, and the results of five independent experiments are summarized in Table 1. First, we find the loop around A330 (in H20, Fig. 3D) with only one protection signal and no interference signals in contrast to the binary complexes (Fig. 3C). Interferences in the loop of H19 are lost and A309, A310, and C314 are rendered protected in the complex. The C302–G303 connection is exposed to iodine cleavage in contrast to either of the binary complexes (Table 1, protection column). A311 interferes with binding, but when the fragment is present

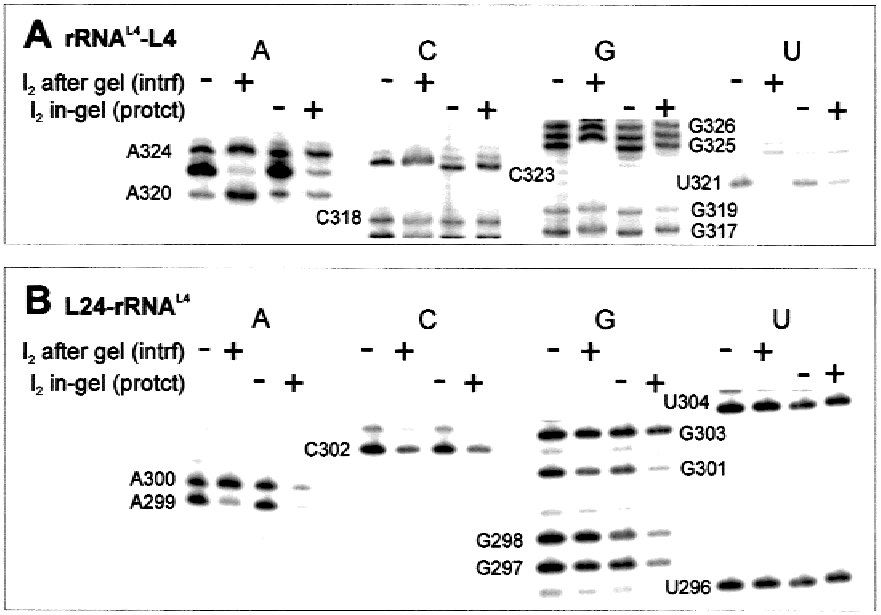

FIGURE 3. Iodine cleavage pattern of phosphorothioated rRNA in complex with protein L4 and L24 (sections of 13% polyacrylamide/urea gels); + and − indicate presence and absence of proteins L4 (**A**) and L24 (**B**). **A:** Regions of interaction with protein L4 (317–326). **B:** Regions of interaction with protein with L24 (296–304).

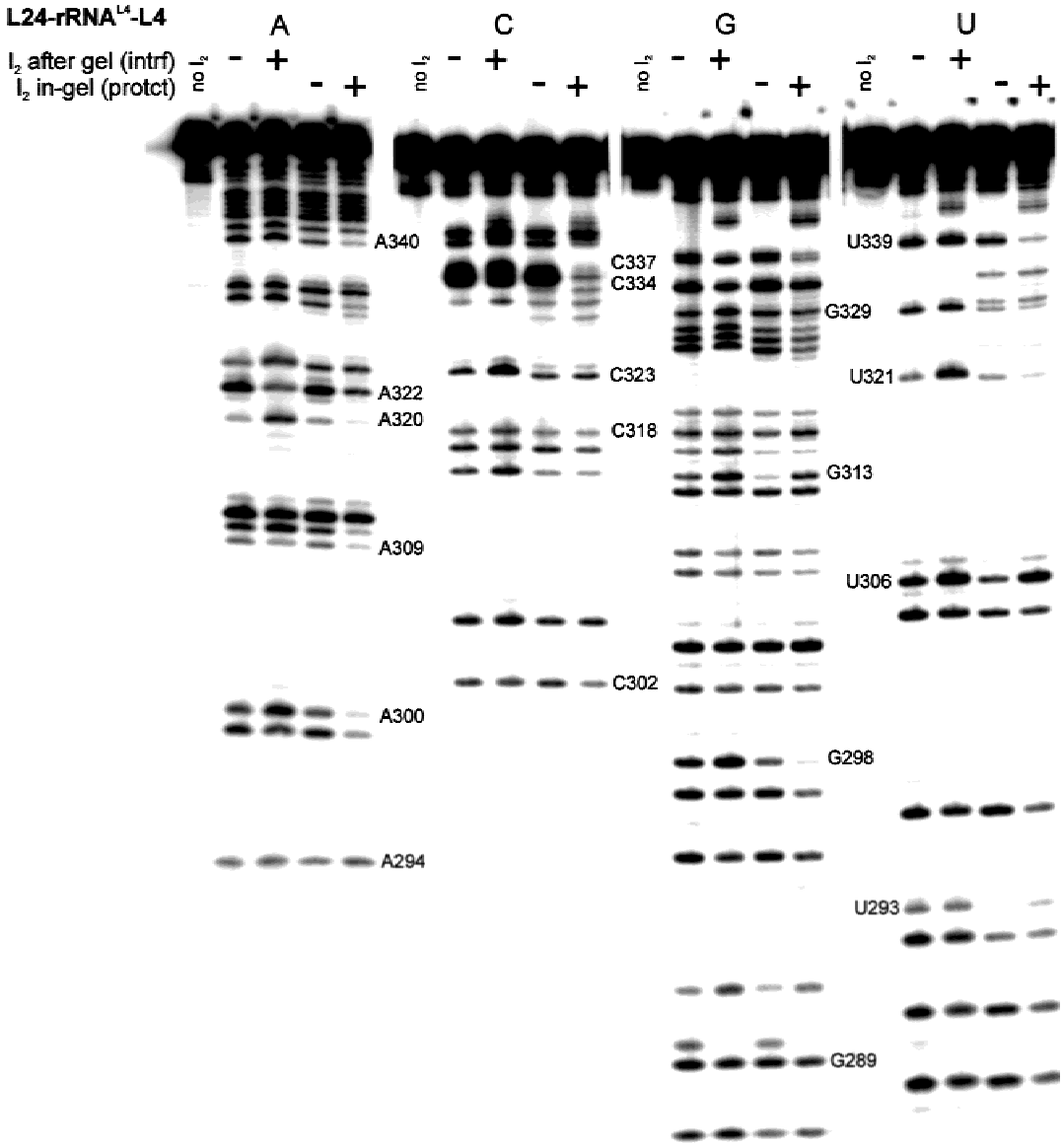

FIGURE 4. Iodine cleavage pattern of phosphorothioated rRNA from the L4–rRNA^{L4}–L24 ternary complex (13% polyacrylamide/urea gel); + and − indicates presence and absence of proteins L24 and L4.

in the complex, the cleavage at A311 is enhanced moderately as in the L24–rRNA^{L4} complex (relative intensity 1.43; Table 1). Surprisingly, 10 additional phosphorothioates spread over the fragment are enriched in the L24–rRNA^{L4}–L4 complex (Fig. 3D, arrows).

Concerning the interaction sites of the two proteins, the A322 interference (L4) is the only one also seen in the ternary complex. This part of the backbone is cleaved efficiently when present in the ternary complex (Fig. 2D, diamond). Interestingly the O-to-S substitution 5′ to U321, which was essentially abolishing L4 binding in the binary complex, is enriched and protected in the ternary complex. As compared to the binary complex, the L24 dependent interferences disappear (G301 and C302) or become sites of protection (G297, A299, and G338). The protections of positions G298 and A300 of the C334–337 region and of A320 and A340 by L24 and L4, respectively, are observed in both the binary and the ternary complexes.

The striking differences seen, for example, in the binding sites of both proteins between the binary complexes and the ternary complex demonstrate that the rRNA fragment undergoes significant conformational changes when going from either binary complex to the ternary complex.

DISCUSSION

The phosphorothioate method provides a tool for the analysis of function, structure, and interactions of nu-

TABLE 1. Quantitative analysis of the cleavage intensities with the L24–rRNA–L4 ternary complex.

Position[a]	Interference[b]	±	Protection[c]	±
G 295	0.71	0.16	1.07	0.05
U 296	0.70	0.10	0.95	0.12
G 297	0.85	0.10	**0.66**	0.12
G 298	**1.50**	0.76	**0.22**	0.21
A 299	0.73	0.15	**0.32**	0.24
A 300	**1.53**	0.56	**0.13**	0.13
G 301	0.79	0.28	0.87	0.24
C 302	0.69	0.18	1.12	0.15
G 303	0.99	0.09	**1.75**	0.15
U 304	0.80	0.23	0.95	0.14
C 305	0.93	0.13	0.96	0.13
U 306	**1.61**	0.43	1.42	0.11
G 307	0.82	0.07	0.76	0.14
G 308	0.77	0.17	0.95	0.11
A 309	0.68	0.29	**0.61**	0.21
A 310	1.12	0.35	**0.44**	0.35
A 311	**0.59**	0.15	1.43	0.40
G 312	0.96	0.30	1.15	0.22
G 313	**2.03**	1.03	0.72	0.09
C 314	1.16	0.49	**0.45**	0.29
G 315	**1.87**	1.07	**0.50**	0.34
C 316	0.81	0.15	1.01	0.24
G 317	**1.62**	0.26	1.23	0.17
C 318	0.94	0.33	0.81	0.32
G 319	**1.54**	0.26	0.77	0.17
A 320	**3.32**	2.42	**0.32**	0.53
U 321	**2.87**	2.03	**0.27**	0.18
A 322	**0.30**	0.10	**1.54**	0.59
C 323	**2.25**	0.73	**0.64**	0.24
A 324	**1.92**	0.79	0.87	0.41
G 325	1.04	0.33	0.70	0.03
G 326	1.26	0.34	0.90	0.08
G 327	1.11	0.25	0.83	0.32
U 328	1.07	0.16	1.00	0.19
G 329	**1.57**	0.34	0.92	0.37
A 330	1.28	0.26	**0.45**	0.20
C 331	1.29	0.32	0.98	0.31
A 332	1.05	0.28	1.23	0.16
G 333	0.80	0.40	1.39	0.56
C 334–337	0.74	0.31	**0.46**	0.3
G 338	0.94	0.28	**0.58**	0.13
U 339	1.02	0.18	**0.35**	0.07
A 340	0.91	0.21	**0.27**	0.12
C 341	1.04	0.23	0.93	0.14
A 342	1.08	0.12	0.67	0.16
C 343	1.23	0.49	1.09	0.07

[a]Position indicates the phosphate 5′ to the nucleotide under focus. Bold positions: the relative intensity of the band differs by a factor of 1.5 from the intensity of the corresponding band of the compared cleavage pattern (i.e., relative intensities ≤0.66 and ≥1.50; these positions are indicated in Fig. 2D).

[b]Interference indicates intensities of the positions of the RNA extracted from the complex in the gel and cleaved *after extraction*, divided by the corresponding intensities of an RNA that was subjected to electrophoresis as free RNA and *cleaved after extraction* from the gel.

[c]Protection indicates intensities of the RNA bands from *in-gel cleaved* complexes divided by the intensities of the corresponding bands of the RNA extracted from the complex in the gel and cleaved *after extraction*. The range of experimental values are indicated as largest deviation (±) from the average of five independent experiments made with two different RNA preparations. We note that four errors in the interference column (G313, G315, A320, and U321) are higher than all others. This is partially due to the high absolute values of the signals.

cleic acids with atomic resolution (Eckstein, 1985; Verma & Eckstein, 1998). R_p-phosphorothioates are statistically incorporated 5′ to one of the four bases by T7 in vitro transcription. Every single substitution can be mapped by separation of the iodine cleavage products on a sequencing gel. The use of phosphorothioate analogs broadens the applicability of the method in that information about other atomic groups than the phosphate residue are generated (Strobel, 1999).

The in-gel cleavage approach presented here is an extension to the well-established probing techniques. It opens the possibility of monitoring assembly steps of multimolecular complexes, if they can be separated by PAGE. RNP complexes in native polyacrylamide gels behave as in solution. For example, in a DNA–RNA polymerase system, it was shown that on- and off-rates are identical to those in solution (Revzin et al., 1986); the same observation holds true for a ribosomal RNA–protein system (Draper et al., 1988). Therefore structural probing within native gels gives reliable information about the solution structure.

Cleavage patterns of the rRNA^{L4} fragment under various conditions

A comparison of the cleavage pattern of noncomplexed RNA extracted from the gel and then cleaved under denaturing conditions (7 M urea) with that of in-gel cleavage of noncomplexed RNA under native conditions reveals only minor differences (compare the second and fourth lanes in Fig. 4). Evidently, the RNA under gel-shift conditions is either not strongly structured or the structure only moderately affects the iodine accessibility. There is one surprising exception, namely position U293, that is not part of the minimal binding site for the proteins (Stelzl et al., 2000a) and cannot be cleaved within the gel. In the *E. coli* 23S rRNA secondary structure, U293 is directly 5′ to an asymmetric internal loop in H18 that consists solely of adenines, and evidently its structure prevents access of iodine to the 5′ phosphate group of U293. This residue is not conserved. Helix 18 is very variable among different species (Egebjerg et al., 1987); for example, an adenine rich internal loop in H18 does not exist in the archaea *Haloarcula marismortui* (Ban et al., 2000).

The regions of the rRNA fragment presumably interacting with the proteins directly match perfectly in a comparison of the probing results of the two techniques, namely, isolation of the complexes from nitrocellulose filter (Fig. 2B; Stelzl et al., 2000a) and in-gel cleavage (Fig. 2C, red and green nucleotides for L4 and L24, respectively). This fact gives credit to the in-gel cleavage variant and allows a precise definition of the interaction sites.

The L4 binding site is presumably represented by the U321 loop, that is, the nucleotides G319–A322 (Stelzl et al., 2000a), and this conclusion is supported by the

following observations. (1) Phosphorothioates 5′ and 3′ to U321 impede binding. (2) The two upstream residues (G319 and A320) are protected from cleavage in the L4–rRNA complex. (3) A 2-nt deletion of C316 and G317 right next to the site was reported that abolishes L4 action in an in vitro competition assay (Zengel & Lindahl, 1993).

The tentative primary binding site of L24 is the region G298–G301 and C337–G338 (Fig. 2C, green nucleotides) as inferred from our previous selection studies (Stelzl et al., 2000a). This conclusion is substantiated by the in-gel phosphorothioate probing data. (1) Phosphorothioate modification of nt A299, G301, and C302 interferes with the L24 binding. (2) L24 protects the RNA backbone at G298 and A300 from reaction with iodine; the O-to-S substitution at A300 favors binding. (3) In the 3′ part of RNA^{L4}, an interesting effect is seen with the phosphorothioated G338 that interferes with binding, whereas the minor bound fraction is exposed to iodine cleavage in the L24 complex. The signals of C334–C337, which cannot be resolved for every base in some experiments, is protected in the L24–rRNA complex. (4) A G298U transversion that increases the affinity of protein L4 to the rRNA fragment abolishes L24 binding (Stelzl et al., 2000a).

Interestingly, only the L24 protections of G298, A300, C334–C337, and A340 and the L4 protection at A320 are similar in the binary and the ternary complexes. All the other signals change qualitatively when we compare the binary complexes with the ternary complex (Fig. 2). Striking differences between binary and ternary complexes are seen. (1) Twelve O-to-S substitutions are enriched in the ternary complex, but only two of these (A300 and A320) were enriched in the binary complexes (Fig. 2D; e.g., U321, C323, A324). Although phosphorothioates are known to increase the affinity for a protein in some cases, the structural meaning is not clear. It could be that sulfur reduces electrostatic repulsion of the oxygen atoms in the RNA backbone if the molecule is packed tightly, because the R_P-sulfur renders the corresponding S_P-oxygen less negative (Dertinger et al., 2000). (2) In the loops of helices 19 and 20 some signals from the binary complexes disappear (e.g., G311, A332), new signals are observed (e.g., U306, A330) and some signals change (e.g., A309, G313). (3) Striking changes are even observed in the protein interaction sites: At the L24 binding site the interferences are either lost (e.g., G301, C302; Fig. 2D) or replaced by protection signals (G297, A299, G338). The phosphorothioate 5′ to U321 that abolishes L4 binding to the RNA becomes protected and, most astonishingly, is now enriched in the ternary complex. (4) Apparently conflicting results are found in the binary complexes for two positions in the L4 binding region: An A320 modification that is enriched in the $rRNA^{L4}$–L4 binary complex but interferes with L24–$rRNA^{L4}$ complex formation is also enriched in the ternary complex. The opposite case is seen with thioated A322, which gives an interference signal in the binary complex with L4 and is enriched in that with L24. In the ternary complex the interference effect is seen; as with L4 alone, thioated A322 also impedes ternary complex formation.

These observations demonstrate an RNA conformational change when going from one of the binary complexes to the ternary complex.

Comparison with the X-ray structure of the 50S subunit from *H. marismortui*

There is a high degree of sequence conservation between the L4/L24 rRNA binding regions in *E. coli* and the archaea *H. marismortui* (Fig. 5A), except that *H. marismortui* contains an additional uridine between G301 and C302 (U308 *H. m.*). In the crystal structure of the *H. marismortui* 50S subunit (Ban et al., 2000), the binding site is a tightly folded structural element (compare the secondary structure with the tertiary structure in Fig. 5A,B, respectively). The rRNA folding brings the two identified protein interaction sites close together and exposes them on opposite sites, with the consequence that the rRNA fragment is sandwiched by the two proteins (Fig. 5C).

Our phosphorothioate data fit well to the structure as seen in the complete subunit: The 5′ part of helix 20 shows hardly any signal and there are no contacts with either protein. The sites of protections are clearly the sites of interaction with the proteins. L4 interacts with a loop structure around U321 (U328 *H. m.*). U321 is flipped out and is like A320 (A327 *H. m.*) not base paired (Fig. 5C, red spheres indicate protections, the yellow sphere indicates A322 interference). Because A340 is protected in the two binary complexes as well as in the ternary complex, we cannot assign the protection to one of the proteins. The same is true for the adjacent U339, which is only protected in the ternary complex. Both residues are shown in violet in Figure 5C.

It is reasonable to assume that *E. coli* helix H18 is extended and that the two L24-binding regions are base paired as is seen in the crystal structure of the 50S subunit from *H. marismortui* (Ban et al., 2000). In the crystal, L24 binds to the major groove of extended H18. Because the R_P-thioates are placed in the major groove of RNA (Rudinger et al., 1992; Cate et al., 1997) the L24-interaction site is nicely mapped by the phosphorothioate probing (Fig. 5C, green and cyan spheres). The corresponding G298 (G304 of *H. m.*) forms a sheared base pair with A340 (A347 of *H. m.*), and thus O6 and N7 of G298 are accessible for L24 from the major groove side. As mentioned above, a G298U transversion increases the affinity of the RNA fragment for L4 but abolishes L24 binding in the respective binary complexes (Stelzl et al., 2000a). The L4 effect indicates that this mutation maintains and obviously stabilizes the RNA structure for L4 binding, because the U can

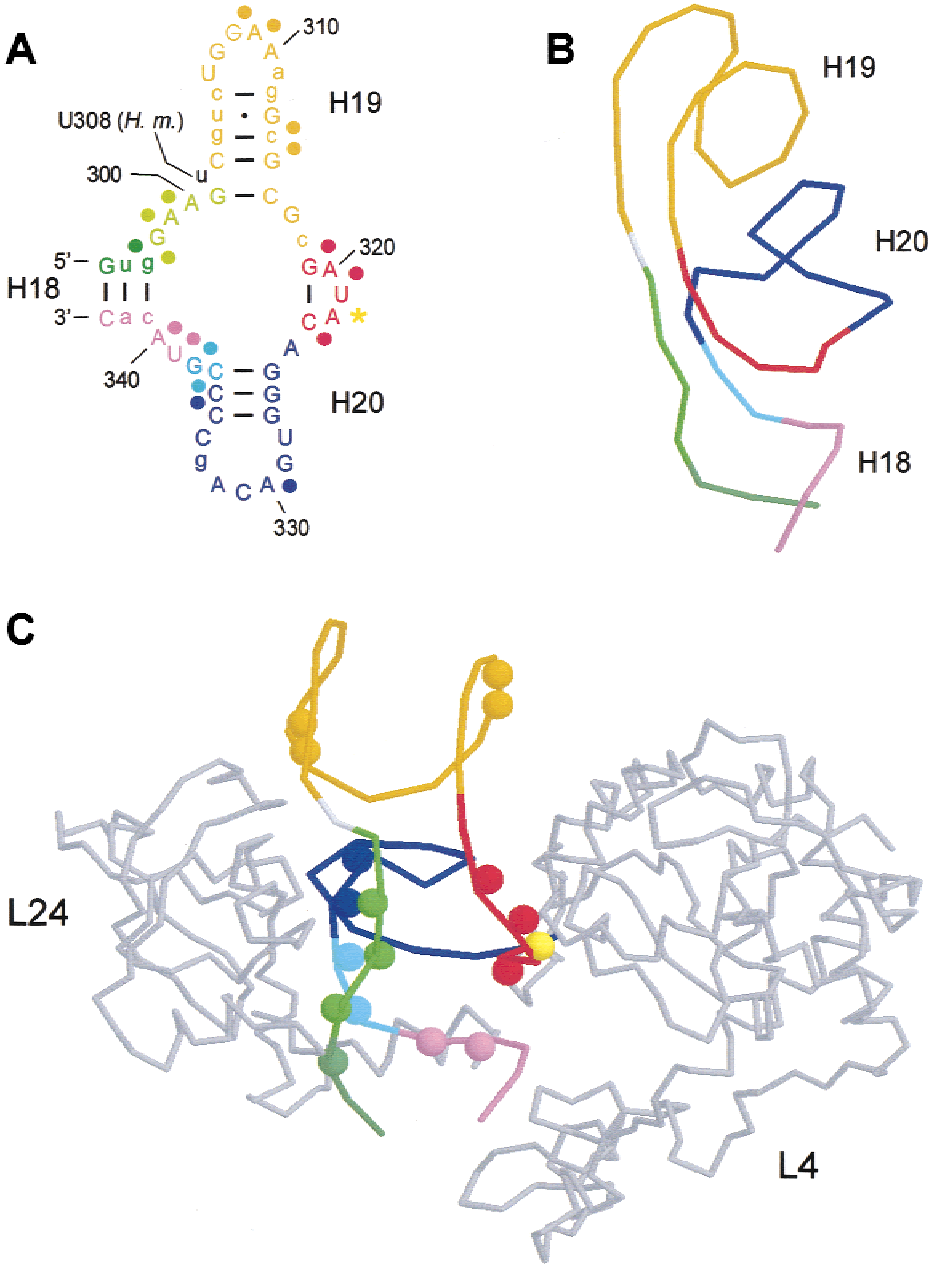

FIGURE 5. A: Secondary structure of the *E. coli* 295–343 region. Bases in capitals are conserved between *E. coli* and *H. marismortui*, small letters indicate *E. coli* sequence. The U between G301 and C302 indicates the additional nucleotide in *H. marismortui.* Iodine cleavage results with the ternary L24–rRNA^{L4}–L4 complex are shown as in Figure 2, but omitting the arrows that indicated increased binding. The color code in **B** and **C** is the same concerning the RNA backbone and the protection sites. **B:** Three-dimensional structure of the RNA backbone from the X-ray structure of the *H. marismortui* 50S subunit (PDB: 1FFK; Ban et al., 2000). **C:** The proteins L4 and L24 bind the rRNA^{L4} region from two different sites (α-C backbone of L24 and L4 in grey; Ban et al., 2000). The L4 interaction site G319–C323 (*H. m.*: G326–C330) is shown in red, and that for L24 in green (G298–G301) and cyan (C337–G338), that is, C304–G307 (*H. m.*) and C344–G345 (*H. m.*), respectively (Ban et al., 2000). In-gel probing results of the L24–rRNA^{L4}–L4 ternary complex are indicated. Pro-R$_P$ oxygen positions, that were protected are shown as spheres according to the color code: G297–A300 in green, A309–A310 and C314–G315 in orange, A330 and C336 in blue, G337–G338 in cyan, U339 and A340 in violet, and A320–C323 in red, except the interference site A322, which is indicated as a yellow sphere.

base pair with A340. If so, the L24 effect means that L24 directly interacts with G298. In such an interpretation, which is quite likely according to the crystal data (Ban et al., 2000), a uridine cannot replace the hydrogen-bonding capacity of G298.

Helices H19 and H20 are bent towards protein L24, so that G307–A330 (G314–A337 of *H. m.*) and G308–G329 (G315–G336 of *H. m.*) in the loops of the helices are base paired (Fig. 5B). The latter base pair forms perfect base stacking interactions with the A502–A487 base

pair (A507–C483 of *H. m.*) located in H24 of domain I distant in the secondary structure map. The presence of protein L24 at this RNA–RNA interaction side agrees well with L24-dependent protections of bases in the 500 region of domain I (site B in Egebjerg et al., 1987). We further note that A309 (A316 *H. m.*) in the loop of H19 base pairs with G1210 (U1314 *H. m.*) in H46 of domain II and that protein L4 has additional contacts to other rRNA strands, in particular to domain II (Ban et al., 2000).

CONCLUSIONS

The present analysis strikingly reveals that the RNA adopts a structure in the ternary complex L24–rRNA–L4 that is different from those seen in either binary complex. Considering the prominent role that both proteins play in early assembly events, the identified short RNA containing the nonoverlapping binding sites of both proteins might be a key element for the 23S rRNA folding during early assembly: L24 is one of the two assembly initiator proteins that bind to the 23S rRNA without the help of other proteins (Nowotny & Nierhaus, 1982). L4 together with L24 belongs to the group of five proteins that are essential and sufficient for the formation of the first assembly intermediate during in vitro assembly of the 50S subunit (Spillmann et al., 1977). This assembly intermediate cannot be bypassed during the formation of active 50S particles (Dohme & Nierhaus, 1976). L24 has no other role, for example, in the functions of the ribosome, because it can be removed from the ribosome after achieving the early assembly intermediate without affecting the further assembly of active 50S subunits (Spillmann & Nierhaus, 1978). This interpretation of in vitro reconstitution experiments is confirmed by in vivo experiments: 23S rRNA deletion variants that lack the $rRNA^{L4}$ region are not incorporated into mature ribosomal particles (Skinner et al., 1985; Liiv et al., 1996), probably because a productive interaction with L24 and L4 is prevented.

The role of L24 in organizing the folding the 23S rRNA is also indicated by the fact that this proteins renders the whole domain I (comprising the sequence 1–560) largely nuclease resistant (Zimmermann, 1980) and stabilizes the structure of this domain (Egebjerg et al., 1987). Although L24 has additional RNA contacts in domain I and L4 is elongated, contacting domains II and V (Gregory & Dahlberg, 1999; Ban et al., 2000), we suggest that the rRNA fragment examined here is one essential trigger for the far-reaching allosteric actions of proteins L24 and L4 on the rRNA folding during early assembly events.

MATERIALS AND METHODS

Preparation of phosphorothioated 5′-[^{32}P] labeled rRNA

T7 in vitro transcription was carried out in 40 mM Tris-HCl (pH 8.0 at 25 °C), 22 mM $MgCl_2$, 5 mM DTT, 1 mM spermidine, 100 μg/mL BSA, 1 U/μL RNasin, 5 U/mL inorganic pyrophosphatase, 3.75 mM of each NTP, 25 μg/mL of purified T7 RNA polymerase, and 35 nM template DNA at 37 °C for 13 h (Triana-Alonso et al., 1995). To statistically incorporate about one NTPαS per molecule into the $rRNA^{L4}$ fragment of *E. coli* 23S rRNA (GG283–U358, 77 nt), the four reactions were supplemented with either 6.5% ATPαS, 8.2% CTPαS, 5.0% GTPαS, or 8.7% UTPαS of the Sp isomers (Amersham). The RNA transcripts were gel purified and 5′-[^{32}P]-labeled. After gel purification, the labeled rRNA was adjusted to a specific activity of about 20,000 dpm/pmol with the corresponding nonlabeled material.

Protein purification

Ribosomal proteins L4 and L24 were purified from total proteins that were acetic-acid extracted from 50S ribosomal particles (Diedrich et al., 1997). L4 is one of the least soluble proteins among the ribosomal proteins from *E. coli*. Therefore, L4 from *Thermus thermophilus* was used in some of the experiments, because the solubility of this protein is better than that from *E. coli* under band-shift conditions. The *T. thermophilus* L4 protein induced the same iodine-cleavage pattern of the rRNA fragment as the corresponding protein from *E. coli*. Purified protein L4 from *T. thermophilus* was a kind gift of A. Rak and M. Garber (Pushchino, Moscow).

Iodine cleavage experiments

Band-shift (Stelzl et al., 2000b)

Eighty picomoles of 5′-[^{32}P]-labeled αS-RNA were heated in 5 μL of binding buffer containing 20 mM HEPES-KOH (pH 7.4 at 0 °C), 4 mM $MgCl_2$, 100 mM NH_4Cl for 1 min at 70 °C and immediately cooled to 4 °C on ice to melt multimers of the RNA. Protein L4 and/or protein L24 (160 pmol each) were incubated in 8 μL binding buffer at 37 °C before mixing with the RNA. For complex formation, the mixture was incubated 15 min at 37 °C and a further 15 min on ice. After the addition of 1.5 μL 78% glycerol, the complex was loaded on a 6% polyacrylamide gel (90 × 60 × 0.7 mm) buffered with the binding buffer and run for 2 h at 80 V. A pump was used to keep the ionic conditions of the running buffer constant. Bands were localized by exposing on a X-ray film (Fuji) for 25–35 min, and cut out accordingly.

Interference experiment

The gel piece was extracted in 200 μL phenol and 200 μL extraction buffer (10 mM Tris-HCl (pH 7.8 at 25 °C), 200 mM NaCl, 1% SDS, 1 mM DTT). RNA was recovered from the aqueous phase by EtOH precipitation in the presence of 1 μg/mL RNase-free glycogen. The RNA was dissolved in 8 μL 7 M urea, and 0.8 μL iodine (50 mM in EtOH) was added on ice for approximately 1 min, following which addition of 1 μL 500 mM DTT stopped the reaction. Cleavage products were separated on a 13% polyacrylamide/urea gel (400 × 300 × 0.4 mm) at 50 W.

In-gel cleavage experiment

The gel piece was soaked in 50 μL of 3 mM iodine in binding buffer on ice for 10 to 15 min. Three microliters of 500 mM DTT were added and the gel piece was further kept on ice for 5 min (the orange color has to disappear completely). A total of 150 μL extraction buffer and 200 μL phenol were added to extract the RNA overnight. After recovery of the RNA via EtOH precipitation (1 μg/mL RNase free glycogen), the RNA was dissolved in 7 M urea and loaded on to a 13% polyacrylamide/urea gel.

In some experiments, the A324 or U328 band was split (see Fig. 4). In principle, different iodine cleavage reaction pathways exist that result in at least two different products: A 3′-cyclic phosphate and a 2′ or 3′ phosphate end, which might be separated by electrophoresis. Splitting of the U328 band was observed in in-gel cleavage experiments only; cleavage at A324 sometimes resulted in two bands even under denaturating conditions in solution.

Specificity of the iodine induced cleavage is controlled by omitting iodine from the experiments. These experiments did not result in any cleavage products (see Fig. 4). RNA that does not contain phosphorothioates is not cleaved by iodine in corresponding experiments either.

Quantitative analysis

The intensity of each band from the gel was quantified with the help of a PhosphorImager system. As described in the legend of Figure 1 and Table 1, interference was calculated by dividing the intensities of the positions of the RNA extracted from the complex in the gel and cleaved *after extraction* by the corresponding intensities of an RNA that was subjected to electrophoresis as free RNA and *cleaved after extraction* from the gel. Division of the intensities of the RNA bands from *in-gel cleaved* complexes by the intensities of the corresponding bands of the RNA extracted from the complex in the gel and cleaved *after extraction* gives protection values. The intensity of each band was normalized by the average ratio of bands that did not change between two lanes under comparison.

ACKNOWLEDGMENT

We thank Sean Connell for continuous help and stimulating discussions.

Received November 12, 2000; returned for revision November 28, 2000; revised manuscript received January 2, 2001

REFERENCES

Ban N, Nissen P, Hansen J, Moore PB, Steitz TA. 2000. The complete atomic structure of the large ribosomal subunit at 2.4 Å resolution. *Science 289*:905–920.

Cate JH, Hanna RL, Doudna JA. 1997. A magnesium ion core at the heart of a ribozyme domain. *Nature Struct Biol 4*:553–558.

Dabrowski M, Spahn CMT, Nierhaus KH. 1995. Interaction of tRNAs with the ribosome at the A and P sites. *EMBO J 14*:4872–4882.

Dabrowski M, Spahn CMT, Schäfer MA, Patzke S, Nierhaus KH. 1998. Contact patterns of tRNAs do not change during ribosomal translocation. *J Biol Chem 273*:32793–32800.

Dertinger D, Behlen LS, Uhlenbeck OC. 2000. Using phosphorothioate-substituted RNA to investigate the thermodynamic role of phosphates in a sequence specific RNA–protein complex. *Biochemistry 39*:55–63.

Diedrich G, Burkhardt N, Nierhaus KH. 1997. Large-scale isolation of proteins of the large subunit from *Escherichia coli* ribosomes. *Protein Express Purif 10*:42–50.

Dohme F, Nierhaus KH. 1976. Total reconstitution and assembly of 50S subunits from *E. coli* ribosomes in vitro. *J Mol Biol 107*:585–599.

Draper DE, Deckman IC, Vartikar JV. 1988. Physical studies of ribosomal protein—RNA interactions. *Methods Enzymol 164*:203–220.

Eckstein F. 1985. Nucleoside phosphorothioate. *Ann Rev Biochem 54*:367–402.

Egebjerg J, Leffers H, Christensen A, Andersen H, Garrett RA. 1987. Structure and accessibility of domain I of *Escherichia coli* 23 S RNA in free RNA, in the L24–RNA complex and in 50 S subunits. Implications for ribosomal assembly. *J Mol Biol 196*:125–136.

Gish G, Eckstein F. 1988. DNA and RNA sequence determination based on phosphorthioate chemistry. *Science 240*:1520–1522.

Gregory ST, Dahlberg AE. 1999. Erythromycin resistance mutations in ribosomal proteins L22 und L4 perturb the higher order structure of 23 S ribosomal RNA. *J Mol Biol 289*:827–834.

Liiv A, Tenson T, Remme J. 1996. Analysis of the ribosome large subunit assembly and 23 S rRNA stability in vivo. *J Mol Biol 263*:396–410.

Malhotra A, Penczek P, Agrawal RK, Gabashvili IS, Grassucci RA, Jünemann R, Burkhardt N, Nierhaus KH, Frank J. 1998. *E. coli* 70S ribosome at 15 Å resolution by cryo-electron microscopy: Localization of fMet-tRNA$_f^{Met}$ and fitting of L1 protein. *J Mol Biol 280*:103–116.

Milligan JF, Uhlenbeck OC. 1989. Determination of RNA–protein contacts using thiophosphate substitutions. *Biochemistry 28*:2849–2855.

Nierhaus KH. 1991. The assembly of prokaryotic ribosomes. *Biochimie 73*:739–755.

Nowotny V, Nierhaus KH. 1982. Initiator proteins for the assembly of the 50S subunit from *E. coli* ribosomes. *Proc Natl Acad Sci USA 79*:7238–7242.

Powers T, Daubresse G, Noller HF. 1993. Dynamics of in vitro assembly of 16S rRNA into 30S ribosomal subunits. *J Mol Biol 232*:362–374.

Powers T, Noller HF. 1995. Hydroxyl radical footprinting of ribosomal proteins on 16S rRNA. *RNA 1*:194–209.

Revzin A, Ceglarek JA, Garner MM. 1986. Comparison of nucleic acid–protein interactions in solution and in polyacrylamide gels. *Anal Biochem 153*:172–177.

Rudinger J, Puglisi JD, Putz J, Schatz D, Eckstein F, Florentz C, Giege R. 1992. Determinant nucleotides of yeast tRNA^{Asp} interact directly with aspartyl–tRNA synthetase. *Proc Natl Acad Sci USA 89*:5882–5886.

Schatz D, Leberman R, Eckstein F. 1991. Interaction of *Escherichia coli* tRNA^{Ser} with its cognate aminoacyl–tRNA synthetase as determined by footprinting with phosphorothioate-containing tRNA transcripts. *Proc Natl Acad Sci USA 88*:6132–6136.

Skinner RH, Stark MJR, Dahlberg AE. 1985. Mutations within the 23S rRNA coding sequence of *E. coli* which block ribosomes assembly. *EMBO J 4*:1605–1608.

Smith JS, Nikonowicz EP. 2000. Phosphorothioate substitution can substantially alter RNA conformation. *Biochemistry 39*:5642–5652.

Spillmann S, Dohme F, Nierhaus KH. 1977. Assembly in vitro of the 50S subunit from *Escherichia coli* ribosomes: Proteins essential for the first heat-dependent conformational change. *J Mol Biol 115*:513–523.

Spillmann S, Nierhaus KH. 1978. The ribosomal protein L24 of *E. coli* is an assembly protein. *J Biol Chem 253*:7047–7050.

Stelzl U, Spahn CMT, Nierhaus KH. 2000a. Selecting rRNA binding sites for the ribosomal proteins L4 and L6 from randomly fragmented rRNA: Application of a method called SERF. *Proc Natl Acad Sci USA 97*:4597–4602.

Stelzl U, Spahn CMT, Nierhaus KH. 2000b. RNA–protein interactions in ribosomes: In vitro selection from randomly fragmented rRNA. *Methods Enzymol 318*:251–268.

Strobel SA. 1999. A chemogenetic approach to RNA function/structure analysis. *Curr Opin Struct Biol 9*:346–352.

Triana-Alonso FJ, Dabrowski M, Wadzack J, Nierhaus KH. 1995. Self-coded 3′-extension of run-off transcripts produces aberrant products during in vitro transcription with T7 RNA polymerase. *J Biol Chem 270*:6298–6307.

Verma S, Eckstein F. 1998. Modified oligonucleotides: Synthesis and strategy for users. *Annu Rev Biochem 67*:99–134.

Voertler CS, Fedorova O, Persson T, Kutzke U, Eckstein F. 1998. Determination of 2′-hydroxyl and phosphate groups important for aminoacylation of *Escherichia coli* $tRNA^{Asp}$: A nucleotide analogue interference study. *RNA 4*:1444–1454.

Zengel JM, Lindahl L. 1993. Domain I of 23S rRNA competes with a paused transcription complex for ribosomal protein L4 of *Escherichia coli*. *Nucleic Acids Res 21*:2429–2435.

Zimmermann RA. 1980. Interactions among protein and RNA components of the ribosome. In: Chambliss G, Craven GR, Davies J, Davis K, Kahan L, Nomura M, eds. *Ribosomes: Structure, function and genetics*. Baltimore: University Park Press. pp 135–169.